THE ASTROPHYSICAL JOURNAL, 443:617–624, 1995 April 20

THE VARIABILITY OF THE DOUBLE-PEAKED BALMER LINES IN THE ACTIVE NUCLEUS OF NGC 1097

THAISA STORCHI-BERGMANN[1]
Departamento de Astronomia, IF-UFRGS, CP 15051, CEP 91501-970, Porto Alegre, RS, Brasil;
thaisa@if1.ufrgs.br

MICHAEL ERACLEOUS,[1] MARIO LIVIO, AND ANDREW S. WILSON[1,2]
Space Telescope Science Institute, 3700 San Martin Drive, Baltimore, MD 21218;
eracleous@stsci.edu, mlivio@stsci.edu, awilson@stsci.edu

ALEXEI V. FILIPPENKO
Department of Astronomy, University of California, Berkeley, CA 94720;
alex@bkyast.berkeley.edu

AND

JULES P. HALPERN
Columbia Astrophysics Laboratory, Columbia University, 538 West 120th Street, New York, NY 10027;
jules@carmen.phys.columbia.edu
Received 1994 June 27; accepted 1994 October 24

ABSTRACT

We present spectroscopic observations of the nucleus of the Seyfert/low-ionization nuclear emission-line region galaxy NGC 1097 spanning the period 1991–1994. The goal was to monitor anticipated variations of the broad, double-peaked Balmer lines which appeared abruptly in 1991. We find that the broad Balmer lines have varied significantly over the monitoring period, both in their integrated fluxes and in their profile shapes. The integrated Hα flux has decreased by a factor of 2, the Hα/Hβ ratio has increased, and the originally asymmetric Hα profile has become symmetric. The decline of the Hα flux and the change in the Hα/Hβ ratio can be interpreted as consequences of either increased obscuration along the line of sight, or a decline in the ionizing continuum, but neither of these scenarios can account for the change in profile shapes. A model attributing the line emission to a precessing elliptical ring around a 10^6 $M_\odot$ nuclear black hole can reproduce the observed profile variations. In this scenario, the line-emitting ring is the result of the tidal disruption of a star by the black hole. Alternative scenarios associating the broad-line emission with a collimated bipolar outflow also remain viable, but binary black holes and inhomogeneous accretion disks are disfavored by the observed pattern of variability.

Subject headings: galaxies: individual (NGC 1097) — galaxies: nuclei — galaxies: Seyfert — line: profiles

1. INTRODUCTION

The barred spiral galaxy NGC 1097 has been known for quite some time to harbor a "mildly" active nucleus whose spectrum (Phillips et al. 1984, and references therein) includes narrow emission lines with relative strengths characteristic of low-ionization nuclear emission-line regions (hereafter LINERS, Heckman 1980). An unusual feature of NGC 1097 is the presence of *two* pairs of faint optical jets straddling the nucleus and extending to distances of about 90 kpc from it (Wolstencroft & Zealey 1975; Arp 1976; Lorre 1978). A recent, most spectacular display by this object was the emergence of double-peaked Balmer lines in 1991 (Storchi-Bergmann, Baldwin, & Wilson 1993, hereafter SBW). The appearance of Seyfert 1 characteristics in the spectrum of NGC 1097 is interesting from many perspectives. Not only can it provide clues about the structure of LINERs and their relation to Seyfert galaxies, but also, the double-peaked Balmer line profiles are reminiscent of the "disklike" emitters found preferentially among broad-line radio galaxies and radio-loud quasars (Eracleous & Halpern 1994). NGC 1097 represents an unusually nearby and bright example of this phenomenon, so it is worthwhile to study its double-peaked Balmer line profiles in detail to test various models of their origin.

As pointed out by SBW and discussed in more detail by Eracleous et al. (1994, hereafter ELHS), models for the origin of double-peaked emission lines abound, and one cannot distinguish between them on the basis of snapshots of the line profiles. Rather, it is necessary to look for profile variations and compare them with detailed model predictions. We have thus undertaken a program of monitoring NGC 1097 spectroscopically in search of variability of its broad Balmer lines. In this paper we present spectra of NGC 1097 spanning a period of $2\frac{1}{4}$ yr and showing significant variability. In § 2 we describe the observations and analysis of the data, and in § 3 we discuss the implications of the observed variability for models of the origin of the double-peaked Balmer lines. In § 4 we present our conclusions and we speculate on possibilities for the future evolution of the properties of NGC 1097.

2. OBSERVATIONS AND ANALYSIS

2.1. *Observations*

Long-slit spectroscopic observations were carried out using a CCD detector on the Ritchey-Chrétien spectrograph at the CTIO 4 m telescope at four epochs, and also with the 3 m

[1] Visiting Astronomer at the Cerro Tololo Inter-American Observatory, which is operated by the Association of Universities for Research in Astronomy, Inc., under a cooperative agreement with the National Science Foundation.

[2] Also Astronomy Department, University of Maryland, College Park, MD 20742.

TABLE 1

JOURNAL OF OBSERVATIONS

Observation Date (UT)	Telescope	Spectral Range (Å)	Slit P.A.	Exposure Time (s)	Spectral Resolution (Å)	Stellar Population and Reddening[a]	Broad Hα Flux[b]
1991 Nov 2[c].....	CTIO 4 m	6195–7069	130°0	2700	1.7	3″6 NW, +0.05	1.95
1992 Oct 5[c]	CTIO 4 m	3200–7000	130°0	685	8.0	3″6 NW	1.94
1993 Sep 12	Lick 3 m	3200–9910	189.0	1200[d]	7.0	3″ NW, +0.07	1.39
1994 Jan 5.....	CTIO 4 m	6195–7069	12.5	1800	1.7	5″ SW, −0.38	1.26
1994 Jan 7.....	CTIO 4 m	3565–6863	139.0	1800	8.0	3″ NW, +0.07	1.29
1994 Feb 17.....	CTIO 4 m	3213–7501	77.0	2400	8.0	3″ NW, +0.07	0.90[e]

[a] The distance and direction from the nucleus from which the stellar population spectrum was extracted, and the reddening correction [$E(B-V)$, in magnitudes] applied to it to match the slope of the nuclear stellar continuum.

[b] In units of 10^{-13} ergs cm^{-2} s^{-1}.

[c] Also presented by SBW.

[d] The exposure time refers to the region of the spectrum around Hα. In other regions the exposure time varies between 600 and 1800 s.

[e] Possibly large uncertainty (see text).

Shane reflector at Lick Observatory on 1993 September 12. A log of the observations is given in Table 1. Spectra were obtained at both medium and low spectral resolution. The medium (1.7 Å) resolution spectra of 1991 November 2 and 1994 January 5 allow a better definition of the Hα profile, while the low (7–8 Å) resolution spectra provide information on the spectral distribution from 3500 to 7000 Å.

The data were reduced in a standard manner using the procedures included in the IRAF software package. Nuclear spectra were extracted from a 2″ × 4″ window centered on the nucleus (1″.5 × 4″ in the case of the 1994 February 17 spectrum). Flux calibration was carried out using spectra of standard stars obtained and reduced in the same way as the spectra of NGC 1097.

2.2. *Comparison of* Hα *Profiles at Different Epochs*

Because not all the nuclear spectra were extracted from windows of the same size and because seeing conditions can affect the flux calibration of individual spectra, spectra obtained at different epochs were normalized to a constant continuum flux at 6800 Å. This is an appropriate normalization scheme because we do not expect any variations of the stellar population spectrum, and we did not find any evidence of a nonstellar continuum in this region of the spectrum. This procedure was adopted instead of the usual normalization according to narrow-line fluxes due to the fact that some of the spectra span a narrow wavelength range around Hα (6200–7000 Å), and hence all the available narrow lines are superposed on the broad Hα line, which introduces an uncertainty in the measurement of their fluxes. The fluxes of the narrow lines in the normalized spectra were measured nevertheless, as a consistency check, and they were found to agree within 15%.

In order to isolate and study the shape of the broad Hα profile, it is necessary to subtract carefully the contribution of the stellar population. To this end, stellar population spectra were extracted from regions 3″–5″ from the nucleus, interior to the star-forming ring (located at about 9″ from the nucleus; Hummel, van der Hulst, & Keel 1987; Storchi-Bergmann, Wilson, & Baldwin 1995). Since the off-nuclear spectra still have (narrow) [O III] λλ4959, 5007, [N II] λλ6548, 6853, and [S II] λλ6717, 6731 in emission, the corresponding regions of the spectra were replaced with a stellar population template from the library of Bica (1988). The stellar population spectra were also corrected for reddening using the Seaton (1979) law in order to match the nuclear continuum shape. The regions from which the stellar population spectra were extracted and the reddening corrections applied to them are given in Table 1.

A comparison of nuclear spectra with the stellar population spectra used to remove the continuum is presented in Figure 1. The residual spectra, shown in the same figure, demonstrate that the subtraction of the stellar population spectra from the nuclear spectra removes the starlight contribution very effectively. The only absorption feature that remains in the residual spectra is the Na I D λ5893 line, which most probably results from excess absorption by interstellar gas in the nucleus. This argues that the difference between the nuclear and off-nuclear stellar population spectra is primarily due to reddening by dust associated with this higher gas column toward the nucleus, rather than with a difference in the stellar populations themselves. Thus the excess Na I D absorption supports the practice of applying reddening corrections to off-nuclear stellar population spectra to match the slope of the nuclear stellar continuum. The spectrum of 1994 February 17 suffers from variations in the spectrograph's spatial focus as a function of wavelength, thereby affecting the relative flux calibration. Consequently, the starlight subtraction was not as satisfactory as in all the other spectra. In addition, the Hα line became intrinsically weak by the time this spectrum was taken. Hence any measurements made from this spectrum are subject to large uncertainties.

In Figure 2 we show the sequence of Hα profiles from 1991 November 2 to 1994 February 17 after subtraction of the underlying starlight contribution. The variation of the broad Hα flux with time is given in the last column of Table 1. The Hα flux did not change significantly (within a typical uncertainty of 5%) between 1991 November 2 and 1992 October 5 (see also SBW), but it decreased by approximately 30% in the following 11 month interval. From 1993 September 12 to 1994 January 7 it decreased by an additional 6% of the initial value, and again, between 1994 January 7 and 1994 February 17, the flux appears to have decreased by about 18% of its original value. However, due to the uncertainties associated with the flux calibration of the most recent spectrum, the magnitude of the latter variation should be regarded with caution.

The shape of the profile changed only slightly in the first 11 month interval, but a significant change became evident in the 1993 September 12 spectrum. The observation of 1994 January 5 shows a profile very similar to that seen on 1993 September

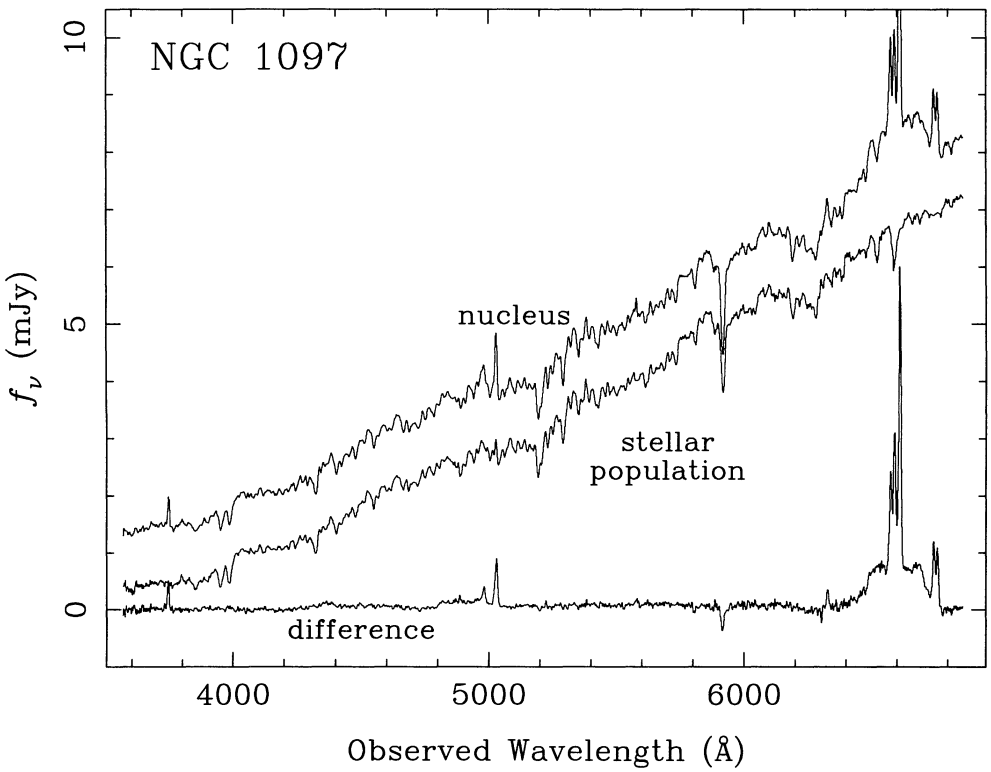

FIG. 1.—A comparison of a recent low-resolution nuclear spectrum of NGC 1097 (average of 1993 September 12 and 1994 January 7 data) with an off-nuclear stellar population spectrum used as a template for the continuum. The residual spectrum shows that the template subtraction removes the stellar absorption features effectively, except for the Na I D λ5893 line, which most probably originates in interstellar gas. There is no evidence for the presence of a featureless continuum. The stellar population spectrum has been shifted downward for clarity.

12. Throughout the $2\frac{1}{4}$ yr spanned by the observations there is no discernible change in the velocity of either of the two peaks. The total variation in the shape of the profile over the monitoring period is illustrated in Figure 3, where we present a comparison between the two medium-resolution spectra of 1991 November 2 and 1994 January 5. The integrated line flux is clearly lower in the later spectrum and the shape of the profile is considerably different. The difference spectrum (also shown in Fig. 3) illustrates clearly that in the $2\frac{1}{4}$ yr between the observations the flux in the red peak has decreased more than the flux in the blue peak, with the result that in 1994 the profile appears to be symmetric.

2.3. *Reddening*

The reddening in the broad-line region can be obtained from the ratio of fluxes of the broad Hα and Hβ lines ($F_{\rm H\alpha}/F_{\rm H\beta}$) under the assumption that the intrinsic value of this ratio remains *constant* at the case B recombination value throughout our observations. The value of $F_{\rm H\alpha}/F_{\rm H\beta}$ measured from the low-dispersion spectra increased from 3.2 ± 0.5 in 1992 October 5 to 4.2 ± 0.7 in 1993 September 12. The latter value was obtained after averaging the 1993 September 12 and 1994 January 7 spectra to improve the signal-to-noise ratio of Hβ (see Fig. 1). The observed difference in Balmer decrement corresponds to a reddening change $\Delta E(B-V) = 0.23 \pm 0.10$ mag, which implies a decrease in the Hα flux by a factor of almost 2, close to the decrease observed. We stress, however, that this interpretation is not unique: the possibility that the observed changes in the Balmer line fluxes and the values of $F_{\rm H\alpha}/F_{\rm H\beta}$ are intrinsic to the source of the emission remains open. We will discuss this and other alternatives further in § 3.1.

The low-dispersion spectrum obtained on 1992 October 5 showed an excess blue continuum at wavelengths shorter than 4000 Å (Fig. 2 of SBW), which is not present in any of the later low-resolution spectra covering this spectral region (see Fig. 1). The "disappearance" of the blue continuum can also be explained by the increased reddening inferred from the values of $F_{\rm H\alpha}/F_{\rm H\beta}$. In particular, the inferred value of $\Delta E(B-V)$ can cause a drop in the flux at 3600 Å by a factor of approximately 4, which would hide the excess blue continuum from our view.

To investigate if the change in Balmer line profiles could be due to an excess reddening of the redshifted peak, we compared the Hα and Hβ profiles after rebinning them to a common velocity scale. This comparison is shown in Figure 4, both for the 1992 October 5 spectrum and the average of the 1993 September 12 and 1994 January 7 spectra. The narrow Hα, [N II] λλ6548, 6583, and [S II] λλ6717, 6731 lines were fitted with Gaussians and subtracted in order to isolate the broad Hα profile. The flux in Hα was then divided by 3.2 in the first spectrum and by 4.2 in the second according to the measured ratios of the Hα and Hβ fluxes. From the residual between the Hβ profile and the scaled Hα profile (also shown in Fig. 4) we conclude that there is no difference between the two profiles within the observational uncertainties. The small discrepancy in the red wing is due to the presence of the [O III] lines redward of Hβ, and a slight mismatch in the same region between the nuclear and off-nuclear stellar population spectra. Consideration of the uncertainties suggests an upper limit of 15% to the relative flux change between the red and blue peaks of Hα that can be attributed to differential reddening. This is much smaller than the observed variation of about 40%, which argues against the possibility that the relative decrease in the

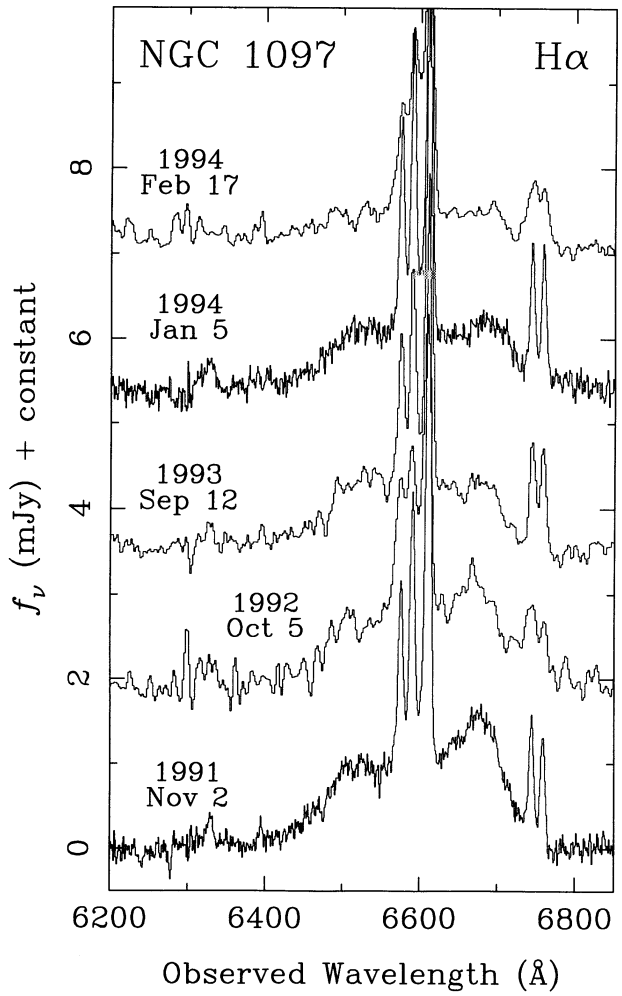

FIG. 2.—The observed broad Hα profiles of the nucleus of NGC 1097 from 1991 November 2 to 1994 February 17. The underlying stellar population spectrum has been subtracted and successive spectra have been shifted vertically (by 1.8 mJy) for clarity.

flux of the red peak is due to an increase in the obscuration of the relevant emitting regions.

3. DISCUSSION

3.1. *The Decline of the Broad Balmer Line Flux*

The variation of the broad Balmer lines of NGC 1097 from 1991 to 1994 comprises both a decline of the integrated line flux and a change in the double-peaked line profile. As demonstrated in § 2.3, the decrease in flux can be attributed to an increase in the obscuration of the broad-line region, which also accounts naturally for the change in the Balmer decrement ($F_{H\alpha}/F_{H\beta}$), and the disappearance of the excess blue continuum observed in 1992 (SBW). In support to this scenario we note the study of variability in three Seyfert galaxies by Goodrich (1989), which has shown that variations in both the broad line and continuum fluxes can be accounted for by changes in the extinction along the line of sight toward the active nucleus.

Another possible explanation for the change in $F_{H\alpha}/F_{H\beta}$ is an intrinsic variation in the source of the line emission. If, for example, the broad-line emission originates in dense, X-ray/UV heated gas, the decline in the line flux may be caused by a decrease in the ionizing flux, which can also explain the disappearance of the excess blue continuum observed by SBW. Furthermore, the decrease in the illuminating flux will cause the effective ionization parameter in the line-emitting region to decrease and hence $F_{H\alpha}/F_{H\beta}$ to increase, since collisional excitation will become more important (see, for example, Wills, Netzer, & Wills 1985). Such an effect is, in fact, observed in Seyfert galaxy monitoring campaigns in which the Balmer decrement is found to steepen as the continuum decreases (e.g., Dietrich et al. 1993; see also the discussion by Shuder 1981, and references therein). Depletion of material from the line-emitting region by accretion onto the central black hole is not a viable explanation for the decline of the Balmer line flux because it would require an unrealistically high accretion rate.

In their simple forms, none of the above mechanisms for the decline of the line flux and the change in $F_{H\alpha}/F_{H\beta}$ can explain the observed change in the *shape* of the Balmer line profiles without a finely tuned variation in the physical conditions of the line-emitting gas. We therefore adopt the hypothesis that the change in the broad-line profiles is not a direct consequence of the mechanism responsible for the decline in the line flux and the increase in $F_{H\alpha}/F_{H\beta}$. In the next section we consider possible scenarios for the origin of the double-peaked Balmer lines and assess their applicability in view of the observed profile variations.

3.2. *Models for the Origin and Variability of the Balmer Lines*

Perhaps the oldest suggestion for the origin of the double-peaked emission lines is the binary black hole hypothesis proposed by Gaskell (1983). In this scenario the two peaks originate in two separate broad-line regions associated with a binary black hole (Begelman, Blandford, & Rees 1980), and the separation between the two peaks is due to the orbital motion of the binary. We consider this to be an unlikely scenario in the particular case of NGC 1097 because (*a*) the line profiles consist of a pair of well-separated peaks, unlike the highly blended profile one would expect to see from a binary black hole system (Halpern & Filippenko 1988; Eracleous & Halpern 1994), and (*b*) the binary black hole scenario is tailored for elliptical galaxies, which are likely to be the product of a merger of two parent galaxies, each with its own nuclear black hole, and it thus difficult to see how a binary black hole would form in the core of a spiral galaxy. Independent of the above arguments, the absence of any changes in the velocities of the two peaks in the $2\frac{1}{4}$ yr of monitoring can be used to constrain the mass of a possible supermassive binary (cf. Halpern & Filippenko 1992). Taken together with the large separation between the two peaks (7250 km s^{-1}, SBW) this implies a lower limit to the total mass of 10^9 $M_\odot$, which is rather large for a mildly active galaxy like NGC 1097, and thus presents a challenge to the binary black hole scenario.

The two most serious contenders among models for the origin of the double-peaked Balmer lines are the bipolar outflow (twin jet) model (Zheng, Binette, & Sulentic 1990; Zheng, Veilleux, & Grandi 1991), and the accretion disk model (Chen, Halpern, & Filippenko 1989; Chen & Halpern 1989). In the former model the two peaks of the line originate in the two oppositely directed streams of the outflow. Since jets are thought to be highly collimated structures, the line emission is most likely a result of the interaction of the jets with interstellar clouds. In models such as those of Zheng et al. (1990), the geometry and velocity field of the outflow are described by arbitrary model parameters which cannot yet be computed from considerations of the detailed physics. Models of this type

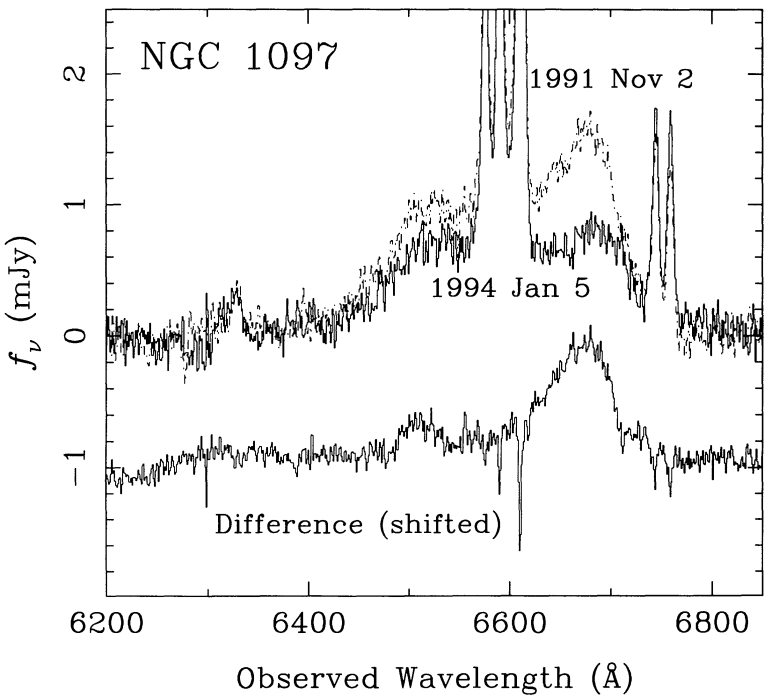

FIG. 3.—Detailed comparison between the two medium-resolution spectra of NGC 1097 obtained in 1991 November 2 (*dashed line*) and 1994 January 5 (*solid line*). The decrease in the integrated line flux and the change in the line profile are unmistakeable. The difference spectrum (shifted downward by 1 mJy for clarity) demonstrates clearly that the flux in the red peak has decreased much more than the flux in the blue peak.

are therefore still ad hoc, and hence flexible enough to reproduce a variety of observed line profiles (for example, the asymmetry between the two peaks can be reproduced by adjusting the relative emissivity of the two jets). This freedom also allows jet models to account for variations in the line profiles by postulating variations in the relevant model parameters (see, for example, the application to 3C 390.3 by Zheng et al. 1991). In spite of this arbitrariness, bipolar outflow still remains an attractive possibility as a source of the double-peaked lines of NGC 1097 because this object already possesses two known pairs of large-scale optical jets. As SBW have speculated, we may be witnessing an episode of ejection of material from the nucleus, which in the distant future may give rise to yet another pair of large-scale jets. In conclusion, we note that if one adopts the specific hypothesis that the line emission originates in a bipolar outflow, but is excited by ionizing radiation from the nucleus, then it is possible to attribute the observed profile variability to reverberation of the line-emitting region in response to a declining ionizing flux. As the ionizing flux decreases, the blue peak will be observed to respond before the red peak due to the difference in light travel times.

The alternative scenario, emission from an accretion disk, has been studied extensively in the context of radio-loud active galactic nuclei (AGNs). The simplest models of homogeneous, circular disks produce line profiles with the blue peak always stronger than the red due to Doppler boosting, which is in contradiction with the observed line profiles of NGC 1097. Models of inhomogeneous disks (e.g., disks with spiral waves or bright spots) or eccentric disks are, in principle at least, promising because they can reproduce asymmetric profiles regardless of the sense of the asymmetry, although the observed pattern of Hα profile variability disfavors inhomogeneous disk models. In the case of disks with spiral waves one would expect to see tertiary peaks moving across the profile (Chakrabarti & Wiita 1994) which are not observed, while in the case of disks with bright spots the lifetime of the profile asymmetries is expected to be of the order of only a few months (ELHS).

The eccentric disk model can reproduce the profile shape quite well and has the potential of explaining the profile variations by invoking precession of the disk. In particular, ELHS were able to fit the 1991 November 2 Hα profile of NGC 1097 with a model attributing the line emission to an elliptical ring (with an eccentricity of 0.5 and a mean pericenter distance of 2600 GM/c^2, where M is the mass of the central object). They suggested that the abrupt appearance of the double-peaked Balmer lines could be due to the recent formation of the ring from the debris released by the tidal disruption of a star. Such events are expected to be quite rare, occurring every 10^4 yr in a given galaxy (e.g., Rees 1988, 1990), but they can release on the order of 1 $M_\odot$ of material which can be accreted within a viscous time (of order 10–100 yr). An approximately equal amount of material will escape capture and will continue along a trajectory away from the black hole (e.g., Evans & Kochanek 1989). ELHS also pointed out that one would expect the line profiles to vary due to precession of the ring, which can occur on a timescale of a few years for a 10^6 $M_\odot$ black hole. In particular, the precession period of the ring estimated by ELHS is

$$P_{\rm GR} \approx 10\, M_6\, \xi_3^{5/2}\ {\rm yr}\,, \qquad (1)$$

where M_6 is the mass of the black hole in units of 10^6 $M_\odot$, and ξ_3 is the pericenter distance of the ring in units of 10^3 GM/c^2.

To investigate whether a precessing elliptical ring can account in detail for the observed variations of the Hα profile, we computed a sequence of model profiles which we present in Figure 5 for comparison with the observed profiles of Figure 2. Throughout this sequence we adopted the best-fit model

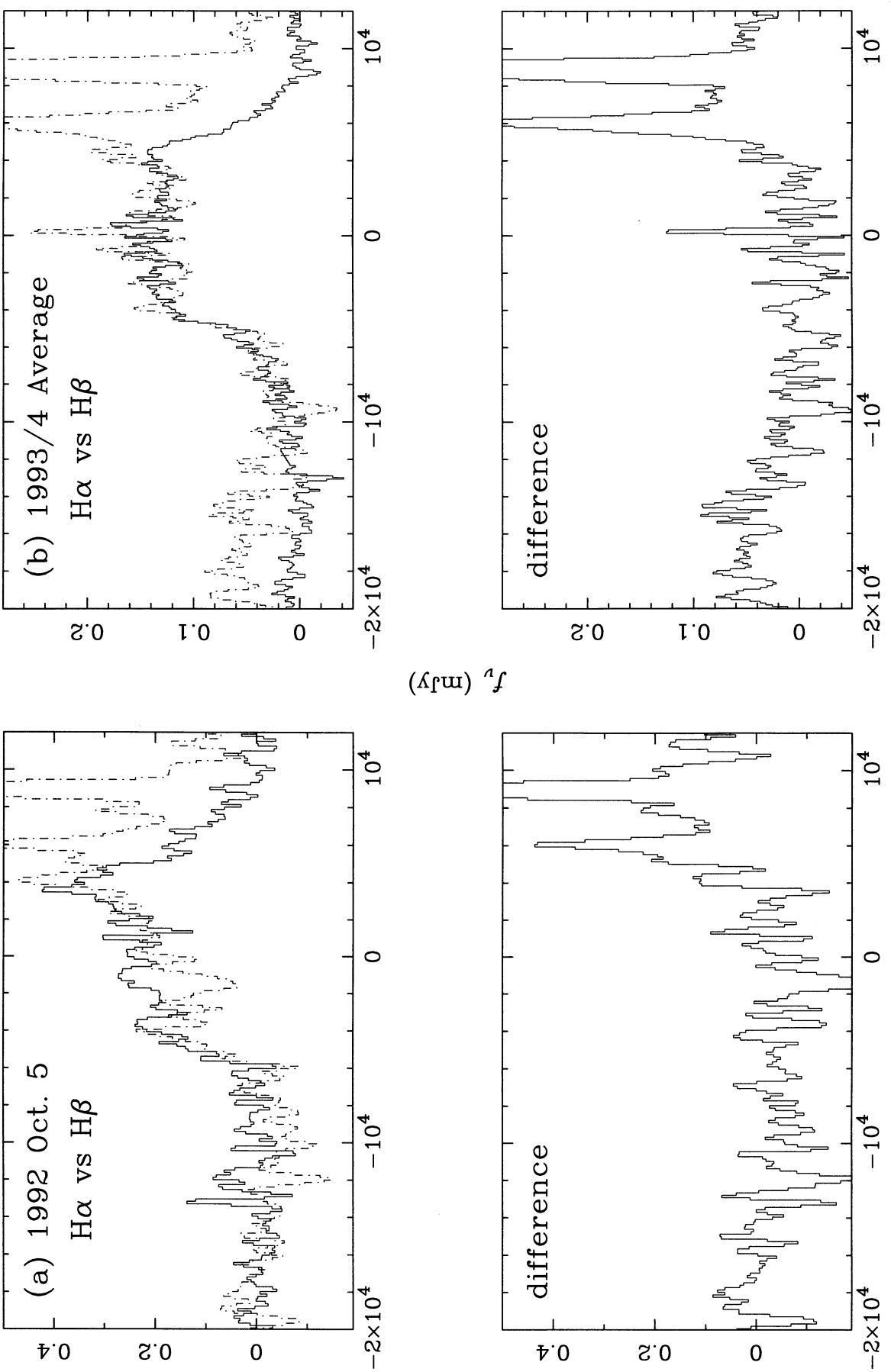

FIG. 4.—Comparison between the broad Hα and Hβ profiles after rebinning them to a common velocity scale: (*a*) from the 1992 October 5 spectrum, and (*b*) from the average of the 1993 September 12 and 1994 January 7 spectra. The Hα profiles are denoted by solid lines, while the Hβ profiles are denoted by dash-dot-dash lines. The narrow Hα, [N II] λλ 6548, 6583, and [S II] λλ6717, 6731 lines have been subtracted from the Hα profiles, and the Hα fluxes renormalized (see § 2.3 for details). The residual of the subtraction of the scaled Hα profile from the Hβ profile is shown at the bottom of each panel.

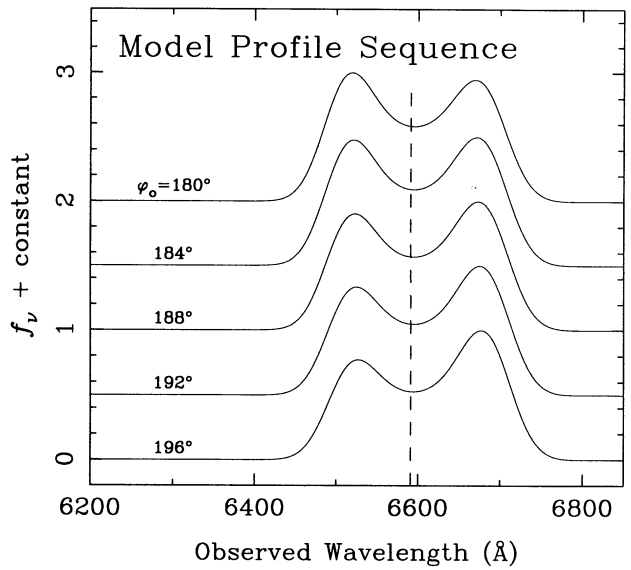

FIG. 5.—A sequence of theoretical profiles computed using the model of an elliptical line-emitting ring described in the text. The model parameter that varies through the sequence is the angle between the major axis of the ring and the line of sight (φ_0). All other models parameters are held fixed at the values determined by ELHS by fitting the 1991 November 2 Hα profile. Successive model profiles have been shifted upward by 0.5 mJy for clarity. All profiles are normalized to unit maximum. The dashed vertical line marks the observed wavelength of the narrow Hα line.

parameters obtained by ELHS in their fit of the 1991 November 2 Hα profile and we varied only the orientation of the major axis of the ring relative to the line of sight (represented by the angle φ_0). The sequence of Figure 5 thus represents the predicted evolution of the line profile due to precession of the elliptical, line-emitting ring. The sequence of model profiles reproduces the observed evolution of the Hα profile shown in Figure 2 fairly well, with only a modest precession of the ring ($\Delta\varphi_0 \approx 16°$). The precession rate appears to be constant, although the quality of some of the observed Hα profiles is not good enough to allow a quantitative test. If the precession is interpreted as a general relativistic advance of the pericenter, then equation (1) implies a mass for the central object of the order of $10^6\ M_\odot$, which is consistent with the low level of nuclear activity observed in NGC 1097. It is also consistent with the suggestion that the ring is the result of the tidal disruption of a star by the black hole, since a black hole with a mass of this order can readily disrupt stars before accreting them (e.g., Rees 1988, 1990).

As a further test of the above scenario, we have estimated the mass of the emitting gas required by the observed Hα luminosity. The estimate was made under the assumption that the dominant Hα emission mechanism is recombination, a reasonable assumption since $F_{H\alpha}/F_{H\beta}$ is close to the recombination value. In our calculation we have adopted the approach and atomic data of Osterbrock (1989). The resulting mass is inversely proportional to the electron density N_e. At a redshift $z = 0.0043$, and using a Hubble constant of $H_0 = 75$ km s^{-1} Mpc^{-1}, the observed Hα flux of 1991 November 2 implies a luminosity $L_{H\alpha} = 7.7 \times 10^{39}$ ergs s^{-1}. The mass of the emitting gas is then

$$M_{H\alpha} \approx 0.24\left(\frac{N_e}{10^8\ \mathrm{cm}^{-3}}\right)^{-1}\left(\frac{H_0}{75\ \mathrm{km\ s}^{-1}\ \mathrm{Mpc}^{-1}}\right)^{-2} M_\odot\,, \quad (2)$$

which can be easily provided by the disruption of a 1 $M_\odot$ star, since about half of the postdisruption debris will remain bound to the black hole. If the density is significantly higher than the value of 10^8 cm^{-3} assumed here, processes such as collisional excitation will begin to contribute to the production of Hα photons, reducing the required amount of gas.

3.3. *NGC 1097 in the Context of Other Double-peaked Emitters*

The spectroscopic survey of more than 90 broad-line radio galaxies and radio-loud quasars by Eracleous & Halpern (1994) has shown radio-loud AGNs to be the preferred hosts of double-peaked Hα lines. A number of additional similarities among the hosts of double-peaked emitters were also uncovered, namely (*a*) Balmer lines which are *on the average* twice as broad as those of typical radio loud AGNs, (*b*) a continuum around Hα which is made up mostly of starlight, which only a small contribution from a nonstellar component, and (*c*) an unusually large equivalent width of low-ionization forbidden lines ([O II] and [S II]) and large [O I]/[O III] ratios compared to typical radio-loud AGNs. These properties, the last two of which are very reminiscent of LINERs, can be understood in the context of the model proposed by Chen & Halpern (1989) in which the inner accretion disk is an ion-supported torus that illuminates the thin outer disk and the narrow-line region with a hard ionizing spectrum. Even though NGC 1097 is not a radio-loud AGN, the abrupt appearance of double-peaked Balmer lines in its spectrum underscores the association of the double-peaked emitters with LINERs, since NGC 1097 now shares all the optical spectral characteristics of double-peaked emitters. This association is strengthened even further by the sudden appearance of double-peaked Balmer lines in the broad-line radio galaxy Pictor A (Halpern & Eracleous 1994; Marziani et al. 1994), whose narrow optical emission lines are nearly LINER like (e.g., Filippenko 1985). The spectral transformation of these two objects suggests that LINERS and double-peaked emitters have more in common than just similar narrow-line ratios and an extremely weak nonstellar continuum. They may share a common excitation mechanism of their narrow-line regions (whatever this may be), which could in turn be related to a common, or at least similar, structure of their central engines. Furthermore, the observed pattern of variability of the Balmer lines in NGC 1097 (and in Pictor A) justifies the practice of treating the double-peaked emission lines as a separate emission component, which varies independently of the "classical" broad lines and probably originates in a region which is dynamically distinct from the classical broad-line region.

4. CONCLUSIONS AND SPECULATIONS

The pattern of variability of the Hα profile provides a powerful constraint for models of the origin of the broad Balmer lines in active galaxies in general, and in NGC 1097 in particular. A scenario involving the tidal disruption of a passing star by a $10^6\ M_\odot$ nuclear black hole and the formation of an elliptical, line-emitting ring from postdisruption debris can explain both the abrupt appearance of the double-peaked Balmer lines and the shapes of their profiles. Moreover, the subsequent precession of the ring can account for the observed profile variations. Elegant as this scenario may appear, it is nevertheless not unique: emission associated with a collimated outflow (a pair of jets) still remains an attractive alternative. However, in view of our currently poor understanding of the formation of jets

and their propagation through the host galaxy, the applicability of this scenario cannot be assessed in detail. The observed variations seriously challenge the binary black hole scenario, which is also disfavored on the basis of arguments presented in § 3.2. Scenarios involving inhomogeneous accretion disks with spiral waves or "bright spots" also appear unlikely.

The tidal disruption picture can provide plausible explanations for the decline of the broad Balmer line fluxes and the steepening of the Balmer decrement, and also allows one to speculate about the future evolution of the lines. If the decline in the line flux is attributed to obscuration, then the obscuring material may be the unbound portion of the postdisruption debris. As this remnant cools, it is conceivable that it can form dust rather quickly (by analogy with the quick formation of dust in nova and supernova ejecta—e.g., Bode & Evans 1989; McCray 1993) and thus it will provide for the observed extinction and reddening. If obscuration is indeed the reason for the decline of the line flux one might expect the lines to recover after the obscuring material moves out of the line of sight. In such a case, the broad lines will reemerge with their blue peak stronger than the red, due to the continuing precession of the hypothesized elliptical ring. Alternatively, if the decline in the line flux is due to a decline in the ionizing continuum (an equally likely possibility), this may suggest that the accretion rate onto the black hole is declining and that the broad lines will eventually disappear completely.

We are indebted to J. Maza for obtaining the 1992 October 5 long-slit spectrum, as well as to T. Matheson and L. C. Ho for assistance with the Lick observations and data reductions, respectively. We also thank K. Korista, B. Peterson, and the referee R. W. Goodrich for very useful comments and suggestions. T. S. B. acknowledges the hospitality of the Space Telescope Science Institute (STScI) and partial support from the Brazilian institutions CNPq, CAPES, and FAPERGS. M. L. and M. E. acknowledge support from NASA under grant NAGW-2678 and from the Director's Discretionary Research Fund at STScI. A. S. W. thanks NASA for support under grants NAGW-2689, NAGW3268, and NAG8-793. A. V. F. acknowledges the support of NSF grant AST-8957063.

REFERENCES

Arp, H. C. 1976, ApJ, 207, L147
Begelman, M. C., Blandford, R. D., & Rees, M. J. 1980, Nature, 287, 307
Bica, E. 1988, A&A, 195, 76
Bode, M. F., & Evans, A. 1989, in Classical Novae, ed. M. F. Bode & A. Evans (Chichester: Wiley), 163
Chakrabarti, S., & Wiita, P. J. 1994, ApJ, 434, 518
Chen, K., & Halpern, J. P. 1989, ApJ, 344, 115
Chen, K., Halpern, J. P., & Filippenko, A. V. 1989, ApJ, 339, 742
Dietrich, M., et al. 1993, ApJ, 408, 416
Eracleous, M., & Halpern, J. P. 1994, ApJS, 90, 1
Eracleous, M., Livio, M., Halpern, J. P., & Storchi-Bergmann, T. 1995, ApJ, 438, 610 (ELHS)
Evans, C. R., & Kochanek, C. S. 1989, ApJ, 346, L13
Filippenko, A. V. 1985, ApJ, 289, 475
Gaskell, C. M. 1983, in Quasars and Gravitational Lenses, Proc. 24th Liège Astrophysical Colloquium (Liège: Institut d'Astrophysique, Univ. Liège), 473
Goodrich, R. W. 1989, ApJ, 340, 190
Halpern, J. P., & Eracleous, M. 1994, ApJ, in press
Halpern, J. P., & Filippenko, A. V. 1988, Nature, 331, 46
———. 1992, in Testing the AGN Paradigm, ed. S. S. Holt, S. G. Neff & C. M. Urry (AIP Conf. Proc. 254), 57
Heckman, T. M. 1980, A&A, 87, 152
Hummel, E., van der Hulst, J. M., & Keel, W. C. 1987, A&A, 172, 32
Lorre, J. J. 1978, ApJ, 222, L99
Marziani, P., Sulentic, J. W., Keel, W. C., Zwitter, T., & Calvani, M. 1994, BAAS, 26, 874
McCray, R. 1993, ARA&A, 31, 175
Osterbrock, D. E. 1989, Astrophysics of Gaseous Nebulae and Active Galactic Nuclei (Mill Valley: University of Science Books), 327
Phillips, M. M., Bagel, B. E. J., Edmunds, M. G., & Díaz, A. 1984, MNRAS, 210, 701
Rees, M. J. 1988, Nature, 333, 523
———. 1990, Science, 247, 817
Seaton, M. 1979, MNRAS, 187, 73P
Shuder, J. M. 1981, AJ, 86, 1595
Storchi-Bergmann, T., Baldwin, J. A., & Wilson, A. S. 1993, ApJ, 410, L11 (SBW)
Storchi-Bergmann, T., Wilson, A. S., & Baldwin, J. A. 1995, in preparation
Wills, B. J., Netzer, H., & Wills, D. 1985, ApJ, 288, 94
Wolstencroft, R. D., & Zealey, W. J. 1975, MNRAS, 173, 51P
Zheng, W., Binette, L., & Sulentic, J. W. 1990, ApJ, 365, 115
Zheng, W., Veilleux, S., & Grandi, S. A. 1991, ApJ, 381, 418